N-tert-butoxycarbonyl (BOC) protected [V 6 O 13 (OCH 2) 3 CNH 2 2] 2− : synthesis, structural characterization, and solution behavior

Ibrahima Fa Bamba, Clement Falaise, Gildas Gbassi, Patrick Atheba, Mohamed Haouas, Emmanuel Cadot

N-tert-butoxycarbonyl (BOC) protected $[V_6O_{13}\{(OCH_2)_3CNH_2\}_2]^{2-}$: synthesis, structural characterization and solution behaviour

Ibrahima Fa Bamba,[a] Clément Falaise,[a] Gildas K. Gbassi,[b] P. Atheba,[b] Mohamed Haouas,[a] Emmanuel Cadot*[a]

[a] *Institut Lavoisier de Versailles, CNRS, UVSQ, Université Paris-Saclay, Versailles, France*

[b] *UFR Sciences Pharmaceutiques et Biologiques (UFR SPB), Université Félix Houphouet Boigny (UFHB)*

To be submitted to J. Coord. Chem.

Enbo Wang Special Memorial Issue

Version June, 29th 2020

Abstract

Herein, we report the synthesis of N-tert-butoxycarbonyl (BOC) protected $[V_6O_{13}\{(OCH_2)_3C\text{-}NH_2\}_2]^{2-}$ built from the Lindqvist-type hexavanadate. The reaction of di-tert-butyl dicarbonate (BOC_2O) with tris(hydroxymethyl)aminomethane (Tris) led to the organic derivative $[(OCH_2)_3C\text{-}NH(BOC)]$ that reacts with the decavanadate in dimethylacetamide (DMA) to form the $[V_6O_{13}\{(OCH_2)_3C\text{-}NH(BOC)\}_2]^{2-}$ anions. The tetrabutylammonium (TBA^+) salt of this hybrid polyoxovanadate, $TBA_2[V_6O_{13}\{(OCH_2)_3C\text{-}NH(BOC)\}_2]\cdot 2DMA$, has been characterized in the solid-state by single crystal X-ray diffraction and infrared spectroscopy, and in solution by multinuclear (^1H, ^{13}C and ^{51}V) and DOSY NMR, and UV-visible spectroscopy.

Keywords

Polyoxovanadate, Hybrid, X-ray structure, NMR, Diffusion ordered spectroscopy, BOC

1. Introduction

The need of redox-active molecular components to develop functional systems relevant in the field of energy has led to a renewal of interest for the chemistry of the polyoxovanadates (POVs). POVs, that represent a sub-class of the polyoxometalates (POMs), are anionic molecular oxides exhibiting a rich structural chemistry due to the ability of the vanadium to adopt different oxidation states (V^{IV} and V^{V}) and coordination geometries such as [VO_4], [VO_5] or [VO_6] [1, 2]. The growing interest for POVs is mainly due to their striking redox and catalytic properties making POVs particularly appealing for both fundamental and applied studies related to the redox-flow batteries [3-6], the lithium or sodium-ion batteries [7-10], the water oxidation catalysis [11, 12] or photocatalysis [13]. Recently, it was also demonstrated that POVs constitute also excellent models to study the intriguing properties of vanadium solid-state oxides [14-16].

Another attractive feature of POVs is their propensity to form a wide variety of covalent organic-inorganic hybrids, offering a way to i) tune the POV properties, and ii) integrate POVs into functional systems or material [17, 18]. The most studied hybrid POVs are the bis(triol-ligands)-substituted Lindqvist-type hexavanadates, *trans*-$[V_6O_{13}\{(OCH_2)_3CR\}_2]^{2-}$, that exhibit fascinating redox [19, 20], supramolecular [21-24] and photochemical [25] properties. In the early 90's, the pioneered work of Zubieta demonstrated that reaction of various Triol-ligands with decavanadate anion $[V_{10}O_{28}]^{6-}$ in acetonitrile led to the formation of $[V_6O_{13}\{(OCH_2)_3C\text{-}R\}_2]^{2-}$ with various functional groups R = NO_2, CH_2OH, CH_3 [19, 26, 27]. Latter Müller reported the pentaerythritol derivatives (R = CH_2OH) can be also prepared in high yield from aqueous mixtures [28]. The $[V_6O_{13}\{(OCH_2)_3C\text{-}CH_2OH\}_2]^{2-}$ anion has been used as platform for various post-functionalization [29, 30]. The use of -NH_2 as functional group is also convenient for post-functionalization of POMs [17, 21, 22, 31, 32], however it is difficult to obtain the $[V_6O_{13}\{(OCH_2)_3C\text{-}NH_2\}_2]^{2-}$ anion by reacting tris(hydroxymethyl)aminomethane (Tris) with vanadate precursors. Indeed the direct reaction of Tris with decavanadate in dry dimethylacetamide (90 °C overnight) led to the desired compound with a very low yield (< 6%) [21]. To tackle this issue, the group of Wei successfully isolated the $[V_6O_{13}\{(OCH_2)_3C\text{-}NH_2\}_2]^{2-}$ anion in good yield (53%) employing a two-step process strategy. First, the amino group is protected with 4-anisaldehyde prior to grafting reaction and then hydrolysis of formed imine is achieved to recover the amine function [33].

Alternatively, N-tert-butoxycarbonyl group (BOC) is now ranked as "one of the most commonly used protective groups for amines".[34]. Such BOC-based methodology derives from that reported by Wei et al. but in this case, the organic precursor corresponding to the BOC-protected Tris compound is synthesized straightforwardly in methanol through a one-pot procedure leading to a 100% yield while the oxazolidine derivatives were obtained from toluene with a lower yield (about 60%) after purification. [35] Then, we show that synthesis methodology based on BOC protecting group

corresponds to an efficient and straightforward route to get the Tris-substituted Lindqvist POV $[V_6O_{13}\{(OCH_2)_3C\text{-}NH_2\}_2]^{2-}$ in good yield (50%). The novel hybrid anion, $[V_6O_{13}\{(OCH_2)_3C\text{-}NH(BOC)\}_2]^{2-}$, isolated as tetra-n-butylammonium (TBA^+) salt has been characterized by single-crystal X-ray diffraction, infrared, UV-vis and multinuclear NMR (^1H, ^{13}C and ^{51}V) spectroscopy.

2. Experimental part

2.1. Materials

All chemicals were used as received without any further treatment. The precursors $(TBA)_3[H_3V_{10}O_{28}]$ and tert-butyl N-[1,3-dihydroxy-2-(hydroxymethyl)propan-2-yl]carbamate were synthesized and characterized following published procedures [36, 37].

2.2. Preparation of $TBA_2[V_6O_{13}\{(OCH_2)_3C\text{-}NH(BOC)\}_2]\cdot 2DMA$

6.24 g of $TBA_3[H_3V_{10}O_{28}]$ (3.7 mmol) and 2.49 g of tert-butyl N-[1,3-dihydroxy-2-(hydroxymethyl)propan-2-yl]carbamate (11.2 mmol) were dissolved in 75 ml of N,N-Dimethylacetamide (DMA). The resulting orange solution was heated at 80 °C for 48 hours. After cooling to room temperature, the slow diffusion of the solution (red-orange) in ether led to the formation of 5 g of red needles of $TBA_2[V_6O_{13}\{(OCH_2)_3C\text{-}NH(BOC)\}_2]\cdot 2DMA$ (notated **V_6-Tris-BOC**) which are then isolated by filtration and dried in air. Yield: 50% based on vanadium.
Anal. Calcd.(found) for $C_{56}H_{122}N_6O_{25}V_6$: C, 42.4(42.3); H, 7.7(7.4); N, 5.3(5.1); V, 19.3(18.9).

2.3. Preparation of $Na_2[V_6O_{13}\{(OCH_2)_3C\text{-}NH(BOC)\}_2]\cdot 6H_2O$

500 mg of $TBA_2[V_6O_{13}\{(OCH_2)_3C\text{-}NH(BOC)\}_2]\cdot 2DMA$ (0.31 mmol) were dissolved in 10 ml of acetonitrile. Then this reddish solution was dropped into 5 mL of acetonitrile containing 2 g of sodium perchlorate hydrate (16 mmol) under stirring. Immediately after the addition of the first drops, a dark orange precipitate was formed. The resulting mixture is stirred for 2 hours. 350 mg of $Na_2[V_6O_{13}\{(OCH_2)_3C\text{-}NH(BOC)\}_2]\cdot 6H_2O$ (0.27 mmol) is recovered by centrifugation (5000 rpm), and washed with acetonitrile and diethyl ether. Yield: 87% based on vanadium.
Anal. Calcd.(found) for $C_{18}H_{44}N_2Na_2O_{29}V_6$: C, 19.7(18.6); H, 4.0(4.25); N, 2.5(2.6); Na, 4.16(3.97);V, 27.7(25.7).

2.4 Preparation of $[V_6O_{13}\{(OCH_2)_3C\text{-}NH_3)\}_2]\cdot 2H_2O$

350 mg of $Na_2[V_6O_{13}\{(OCH_2)_3C\text{-}NH(BOC)\}_2]\cdot 6H_2O$ was dissolved in 15 mL of water, then 5.5 mL of concentrated HCl (37%) were slowly added, provoking the formation of a reddish precipitate. After one day of stirring, the resulting solid is recovered by centrifugation and washed twice with acetonitrile. The dried solids were added to about 10 mL of DI water and ammonia aqueous solution

(25%) was added to obtain a clear solution (pH ~ 9). The evaporation of this solution led to the crystallization of compound $[V_6O_{13}\{(OCH_2)_3C\text{-}NH_3)\}_2]\cdot 2H_2O$. Single crystal X-ray diffraction reveals that the crystal exhibit the same unit cell than the compound reported previously by Wei and co-worker [34].

2.5. Single-crystal X-ray diffraction

Crystal of compound **V_6-Tris-BOC** was selected under polarizing optical microscope and glued in paratone oil. X-ray intensity data were collected at low temperature (T = 220(2) K) on a Bruker D8 VENTURE diffractometer equipped with a PHOTON III C14 using a high brilliance IμS microfocus X-ray Mo Kα monochromatized radiation (λ = 0.71073 Å). Data reduction was accomplished using SAINT V7.53a. The substantial redundancy in data allowed a semi-empirical absorption correction (SADABS V2.10) to be applied, on the basis of multiple measurements of equivalent reflections. Using Olex2 [38], the structure was solved with the ShelXT [39] structure solution program using Intrinsic Phasing and refined with the ShelXL [40] refinement package using Least Squares minimization. The remaining non-hydrogen atoms were located from Fourier differences and were refined with anisotropic thermal parameters. Positions of the hydrogen atoms belonging to $[V_6O_{13}\{(OCH_2)_3C\text{-}NH(BOC)\}_2]^{2-}$ unit, TBA^+ or DMA were calculated and refined isotropically using the gliding mode. Crystallographic data for single-crystal X-ray diffraction studies are summarized in Table 1. These data can be obtained free of charge from The Cambridge Crystallographic Data Centre via https://www.ccdc.cam.ac.uk/structures-beta/. Deposit number: 2006943.

Table 1. Crystal data and structure refinement for **V_6-Tris-BOC**

Empirical formula	$C_{58}H_{122}N_6O_{25}V_6$	ρ_{calc}g/cm^3	1.388
Formula weight	1607.23	F(000)	1696
Temperature/K	220	Crystal size/mm^3	0.16 × 0.14 × 0.12
Crystal system	monoclinic	Radiation	MoKα (λ = 0.71073)
Space group	$P2_1/c$	2Θ range for data collection/°	4.674 to 55.77
a/Å	14.8061(3)	Index ranges	-19 ≤ h ≤ 19 -14 ≤ k ≤ 14 -31 ≤ l ≤ 31
b/Å	10.8895(3)	Reflections collected	81909
c/Å	24.3085(6)	Independent reflections	9131 R_{int} = 0.0399 R_{sigma} = 0.0192
α/°	90	Data/restraints/parameters	9131/0/440
β/°	101.0590(10)	Goodness-of-fit on F^2	1.083
γ/°	90	Final R indexes [I ≥ 2σ (I)]	R_1 = 0.0501 wR_2 = 0.1364

Volume/Å^3	3846.50(16)	Final R indexes [all data]	R_1 = 0.0653 wR_2 = 0.1541
Z	2	Largest diff. peak/hole / e Å^{-3}	0.69/-0.45

2.6. NMR studies

The ^{1}H, ^{13}C{^{1}H}, ^{15}N{^{1}H}, and ^{51}V NMR solution spectra were recorded in 5 mm o.d. tubes with a Bruker Avance 400 spectrometer equipped with a BBI probehead. Chemical shifts are referenced to external 1% Me_4Si in $CDCl_3$ (^{1}H and ^{13}C), $MeNO_2$ (^{15}N) and 90% $VOCl_3$ in C_6D_6 (^{51}V). Translational diffusion measurements were performed using Bruker's "ledbpgs2s" stimulated echo DOSY pulse sequence including bipolar and spoil gradients. Apparent diffusion coefficients were obtained using an adapted algorithm based on the inverse Laplace transform stabilized by maximum entropy [41].

2.7. Fourier transform infrared

Fourier Transform Infrared (FT-IR) spectra were recorded on a 6700 FT-IR Nicolet spectrophotometer, using diamond ATR technique. The spectra were recorded on non-diluted compounds in the range 400-4000 cm^{-1}. ATR correction was applied.

2.8. UV-vis spectra

UV-vis spectra of powder compounds have been collected by using a Perkin-Elmer Lambda 750 spectrophotometer equipped with a powder sample holder set. The UV-vis spectra of solutions were recorded on a Perkin-Elmer Lambda-750 using calibrated 0.2 cm Quartz-cell.

2.9 Elemental analysis

C, H, N Elemental Analysis were carried by BioCIS-UMR 8076 Service Chromato-Masse Microanalyse Faculté de Pharmacie Tour D5-5ème étage 5 avenue JB Clément 92290 CHÂTENAY-MALABRY. Na and V content were determined by Inductively Coupled Plasma optical emission spectroscopy (ICP-AES), using an Agilent 720 Series with axially-viewed plasma and Na/V calibration curve.

3. Results and discussion

3.1. Synthesis

The hybrid hexavanadate $[V_6O_{13}\{(OCH_2)_3C\text{-}NH(BOC)\}_2]^{2-}$ have been prepared in two steps (Figure 1). The first one consists in the preparation of the tert-butyl N-[1,3-dihydroxy-2-(hydroxymethyl)propan-2-yl]carbamate that can be easily prepared in very good yield (100%) from

the reaction of tert-butyloxycarbonyl with di-tert-butyl dicarbonate in methanol [37]. The second synthetic step is inspired by the procedures allowing the formation of the various hybrid Lindqvist-type POV involving the reaction of the decavanadate $(TBA)_3[H_3V_{10}O_{28}]$ with the desired Triol-ligands in hot N,N-dimethylacetamide. Adapting this synthetic route, we prepared in good yield (50 %) the desired compound, as demonstrated by structural characterization, FT-IR spectroscopy, and multinuclear NMR in solution.

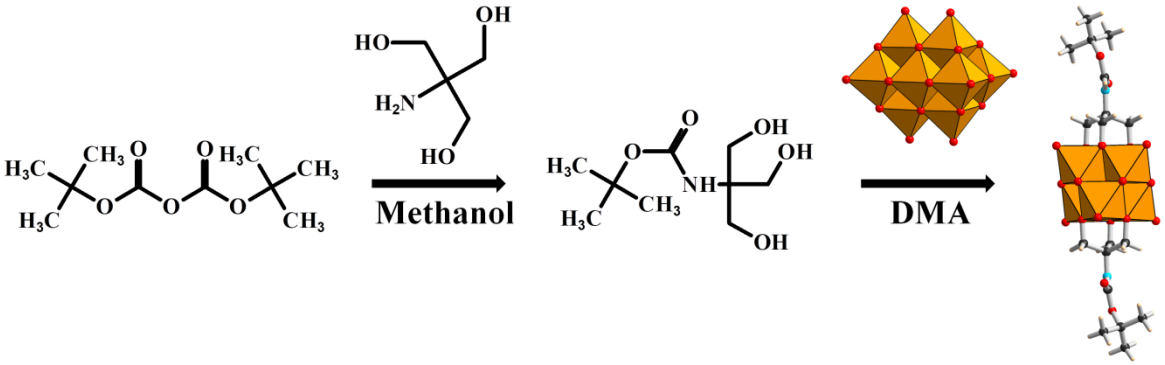

Figure 1. Synthetic pathway leading to the $[V_6O_{13}\{(OCH_2)_3C\text{-}NH(BOC)\}_2]^{2-}$ anion.

3.2. Crystal structure

The compound $(TBA)_2[V_6O_{13}\{(OCH_2)_3C\text{-}NH(BOC)\}_2]\cdot 2DMA$, notated **$V_6$-Tris-BOC**, crystallizes in the centrosymmetric space group $P2_1/c$ and the asymmetric unit contains the half of the hybrid hexavanadate $[V_6O_{13}\{(OCH_2)_3C\text{-}NH(BOC)\}_2]^{2-}$, one TBA^+ cation and one dimethylacetamide molecule of crystallization. The structure of the $[V_6O_{13}\{(OCH_2)_3C\text{-}N\ H(BOC)\}_2]^{2-}$ anion, shown in Figure 2, corresponds to the archetypical Lindqvist-type polyanion in which the six vanadium centres form an octahedron and two trialkoxo ligands occupy the opposite faces of the octahedron in *trans*-mode. An inversion centre is located at the central μ_6-oxygen atoms of the POV. Within the inorganic core $\{V_6O_{19}\}^{8-}$, each vanadium adopts a distorted octahedral geometry in which the shortest and longest V-O distances are observed with the terminal oxygen atoms O^t (1.600(2)-1.606(2) Å) and the central μ_6-oxygen atom (2.2251(4)-2.2492(4) Å), respectively. The bond length between the vanadium atoms and bridging μ_2-oxygen atoms is in the range 1.802(2)-1.854(2) Å, while the V-O distances observed with the alkoxy bridging μ_2-oxygen atoms is slightly longer (2.000(2)-2.038(2) Å). The geometric parameters of the inorganic core in **V_6-Tris-BOC** are similar to those previously observed in the equivalent Tris-derivative hexavanadate $[V_6O_{13}\{(OCH_2)_3CNH_2\}]^{2-}$ [33].

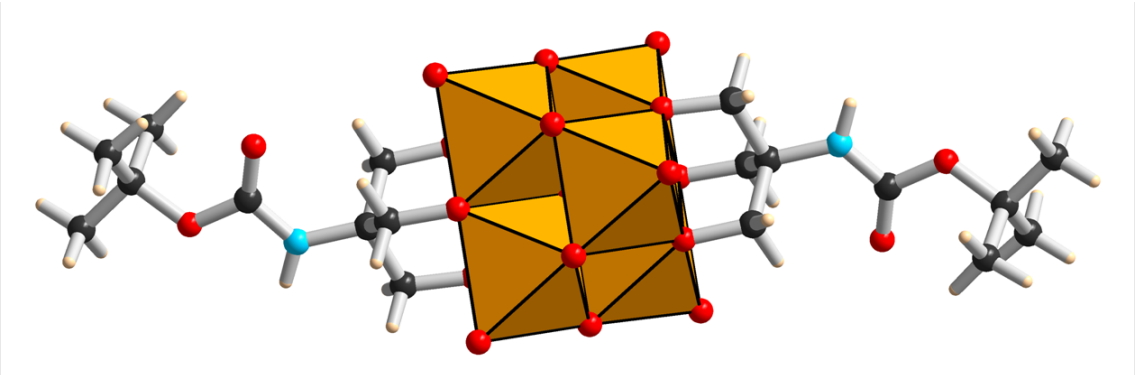

Figure 2. Structural view of $[V_6O_{13}\{(OCH_2)_3C\text{-}NH(BOC)\}_2]^{2-}$ anion. Orange polyhedron: VO_6; red sphere: oxygen ; black sphere: carbon ; blue sphere: nitrogen; light pink sphere: hydrogen

The three-dimensional cohesion is insured mainly by a network of short contacts and hydrogen bonds (Figure 3). The inorganic core of $[V_6O_{13}\{(OCH_2)_3C\text{-}NH(BOC)\}_2]^{2-}$ anion is surrounding by four tetrabutylammonium cations interacting through numerous short contacts ($d_{C\text{-}H\cdots O\text{-}V}$ = 2.38-2.80 Å) between the hydrogen atoms of alkyl tails and the oxygen atoms located at the surface of the $\{V_6O_{19}\}^{8-}$ motif (Figure 3A). Such an organization involves the formation of a neutral chain $\{TBA_2[V_6O_{13}\{(OCH_2)_3C\text{-}NH(BOC)\}_2]\}$ along the *b* axis where the $\{V_6O_{19}\}^{8-}$ motifs are separated by a pair of TBA cations. Such chains are connected together in the *ab* plane by intercalated solvent molecules (DMA) of crystallization (two DMA per POV unit). Each DMA molecule interacts with one POV by one hydrogen bond between the oxygen atom of the DMA and the N-H group of POV ($d_{N\text{-}H\cdots O\text{-}C}$ = 2.221(4) Å) and with another POV by short contact ($d_{C\text{-}H\cdots O\text{-}V}$ = 2.561(2) Å) (Figure 3B). From this organization, it results the formation of layers that are stacked along the *c* axis, with 180° rotation and a shift of *b*/2 from one to the other. The organic tails of the $[V_6O_{13}\{(OCH_2)_3C\text{-}NH(BOC)\}_2]^{2-}$ anion point upward and downward the two adjacent layer planes, generating van der Waals interactions between the layers that ensure the 3D cohesion of the crystal structure (Figure 3C).

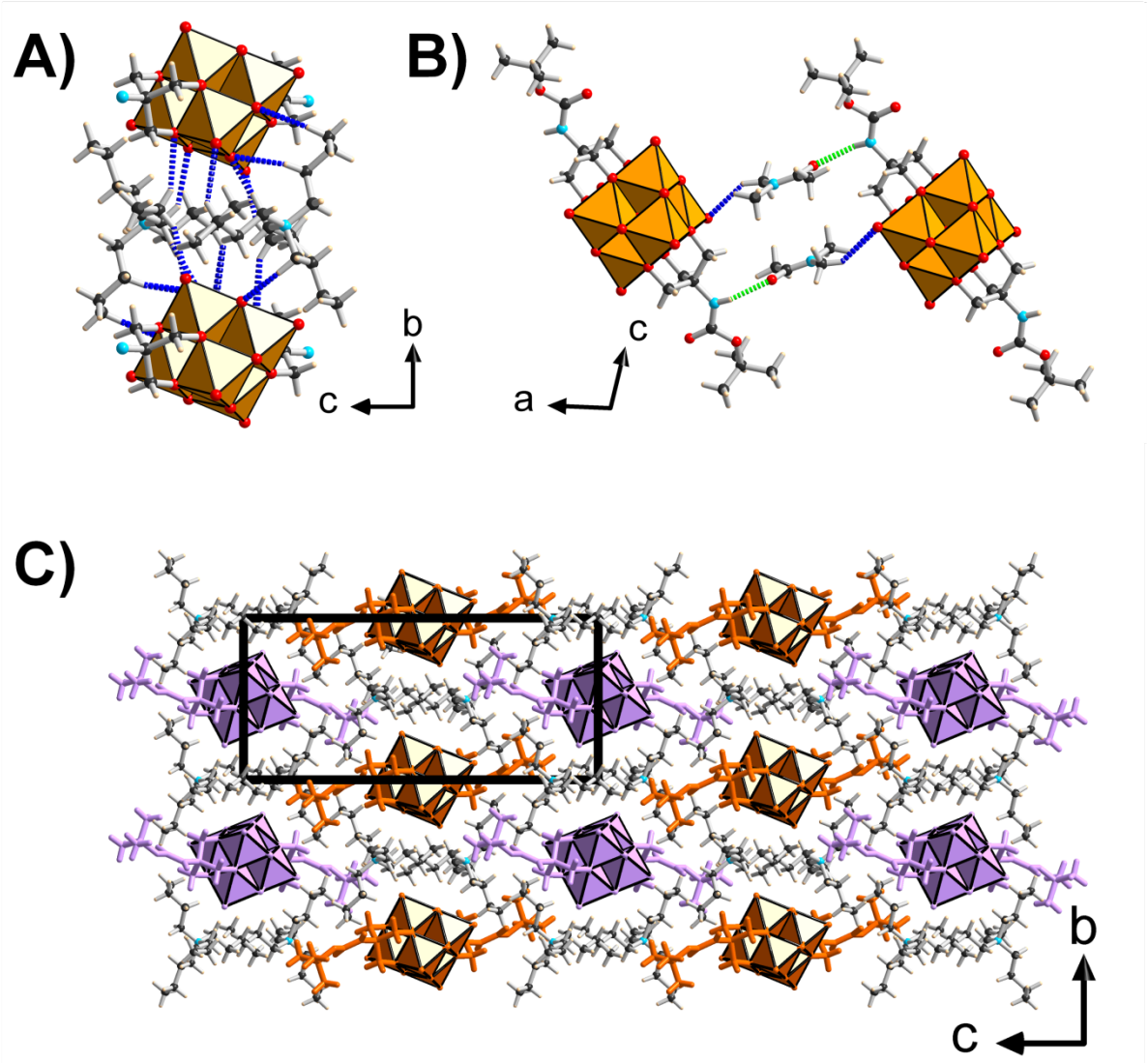

Figure 3: A) Illustration of the short contacts occurring between POVs and TBA^+ cations showing a pair of TBA^+ connecting two POVs along the *b* axis. Doted blue lines: short contacts between the hydrogen atoms of the alkyl chains of TBA^+ and the oxygen atoms located at the surface of the POV. The BOC chain is omitted for clarity. B) Illustration of the supramolecular interaction between the POV and the DMA. Doted green lines: hydrogen bonds between the NH groups of the POV-Tris and the oxygen atom of the DMA. Doted blue lines: short contacts between hydrogen atoms of DMA and terminal oxygen atoms of the POV. C) Illustration of the packing along *a* axis, showing the stacking of the layer along the *c* axis. To highlight the two different layers, two colours have been used for the POVs. DMA molecules have been omitted for clarity.

3.3. FT-IR spectroscopy

The figure S8 shows the FT-IR spectrum of $(TBA)_2[V_6O_{13}\{(OCH_2)_3C\text{-}NH(BOC)\}_2]\cdot 2DMA$. The three characteristic features of the inorganic core $\{V_6O_{19}\}^{8-}$ are located at 949, 805 and 720 cm^{-1}. The strong peak located at 949 cm^{-1} corresponds to the vibration $V{=}O^t$ (terminal oxygen atoms).The two other

peaks are attributed to vibrations of V–O^b–V that involves the bridging oxygen atoms of the metal-oxo framework. Numerous strong IR absorptions of the organic part of the hybrid hexavanadate, the DMA and the TBA cations are observed in the range 1000-1650 cm^{-1}, however the identification of all peaks is challenging. The broad C=O stretching peaks located at 1706 and 1642 cm^{-1} can be attributed to the amid group of the ligand {$(OCH_2)_3$C-NH(BOC)} and the DMA, respectively. The peaks about 1472, 1400, 1370 cm^{-1} are assigned to asymmetric and symmetric deformation of the C–H of the methyl and methylene groups of the TBA cation, the ligand and the DMA. Asymmetric and symmetric vibrations of C-H are observed in the range 2873 and 2964 cm^{-1}.

.*3.4. NMR spectroscopy*

The compound $(TBA)_2[V_6O_{13}\{(OCH_2)_3C\text{-}NH(BOC)\}_2]\cdot 2DMA$ has been characterized by ^1H, $^{13}C\{^1H\}$, and ^{51}V NMR in acetonitrile (ACN). The ^{51}V NMR spectrum (Supporting Information Figure S1) exhibits a single resonance at -497 ppm (half-height line width $\delta\,\nu_{1/2}$ ca. 400 Hz) indicating a highly symmetric POV, consistent with a *trans*-coordination mode. Similar result was observed with $[V_6O_{13}\{(OCH_2)_3C\text{-}N(4\text{-}CONHC_5H_4N)\}_2]^{2-}$ anion (-495 ppm / DMSO-D_6) [20]. The ^1H NMR spectrum (Supporting Information Figure S1) confirms the grafting of organic moieties on the surface of the POV showing the signals of methylenic protons V_6-$(OCH_2)_3$ and methyl groups of the Tris-BOC at 5.16 and 1.38 ppm, respectively. Signals of TBA cations at 0.99, 1.45, 1.60, and 3.16 ppm, and of DMA crystallization solvent at 1.98, 2.84, and 2.97 ppm are also identified. Integration of these signals reveals molar ratios Tris-BOC / TBA / DMA = 1 / 1 / 1, which is consistent with a global POV charge of 2- and co-crystallization of 2 DMAC molecules with one POV unit as determined by XRD analysis. ^{13}C NMR spectrum (Supporting Information Figure S2) shows the resonances of Tris-BOC moieties at 28.3, 52.1, 83.7, 87.2, and 155.5 ppm. The overall NMR data are in agreement with pure and stable compound in acetonitrile.

The compound $(TBA)_2[V_6O_{13}\{(OCH_2)_3C\text{-}NH(BOC)\}_2]\cdot 2DMA$ is not soluble in aqueous solution. However, the exchange of counter cations TBA^+ by sodium allows solubilizing the hybrid POV $Na_2[V_6O_{13}\{(OCH_2)_3C\text{-}NH(BOC)\}_2]\cdot 6H_2O$ in water. Hydrolysis of the peptidic function is therefore achieved in acidic medium using HCl, which provokes an immediate precipitation. The resulted solid consists of the neutral protonated form, $[V_6O_{13}\{(OCH_2)_3C\text{-}NH_3\}_2]$. Figure 5 shows the ^1H NMR spectra of $Na_2[V_6O_{13}\{(OCH_2)_3C\text{-}NH(BOC)\}_2]$ and $[V_6O_{13}\{(OCH_2)_3C\text{-}NH_3\}_2]$ in D_2O. The spectrum of $Na_2[V_6O_{13}\{(OCH_2)_3C\text{-}NH(BOC)\}_2]$ exhibits the signals of CH_2 of Tris moieties at 5.32 ppm and of the methyl groups of the BOC at 1.32 ppm. To verify that the BOC is still attached to the POV upon its dissolution in aqueous solution, DOSY NMR is carried out. The spectrum shown in Supporting Information (Figure S3) reveals that the two organic parts (Tris and BOC) diffuse with the same rate at 295 $\mu m^2/s$. This proves that the Tris-BOC is robust and remains intact in aqueous solution, and then acidic protons are needed to hydrolyse the amide function. The neutral solid product

$[V_6O_{13}\{(OCH_2)_3C\text{-}NH_3\}_2]$ is insoluble in water and deprotonation of ammonium groups is needed to solubilize it. Therefore, NMR measurements were conducted in basic medium ($NaOD/D_2O$). The ^1H NMR spectrum (Figure 5B) shows the signal of CH_2 of the Tris at 5.00 ppm and a small signal at ca. 1.2 ppm accounting for residual BOC. DOSY NMR (Supporting Information Figure S4) confirms the assignments where two distinct diffusion rates are measured at 422 and 758 $\mu m^2/s$ for the POV-Tris and BOC, respectively. ^{13}C NMR (Supporting Information Figures S5 and S6) provides further support of ^1H assignments of $Na_2[V_6O_{13}\{(OCH_2)_3C\text{-}NH(BOC)\}_2]$ and $[V_6O_{13}\{(OCH_2)_3C\text{-}NH_3\}_2]$. To provide a definitive proof of hydrolysis of the amide function, ^{15}N NMR has been carried out. The $^{15}N\{^1H\}$ HMBC (Supporting Information Figure S7) reveals that the initial signal of the amid function in $[V_6O_{13}\{(OCH_2)_3C\text{-}NH(BOC)\}_2]^{2-}$ at -290.7 ppm shifts to -352.8 ppm, corresponding to typical chemical shifts range for amines. Finally, the ^{51}V NMR spectra (Figure 6) of $Na_2[V_6O_{13}\{(OCH_2)_3C\text{-}NH(BOC)\}_2]$ and $[V_6O_{13}\{(OCH_2)_3C\text{-}NH_3\}_2]$ are comparable exhibiting a broad resonance at ca. -507 ppm (half-height line widths $\delta\nu_{1/2}$ ~ 500-1000 Hz). This signature is typical of Lindqvist type structure.

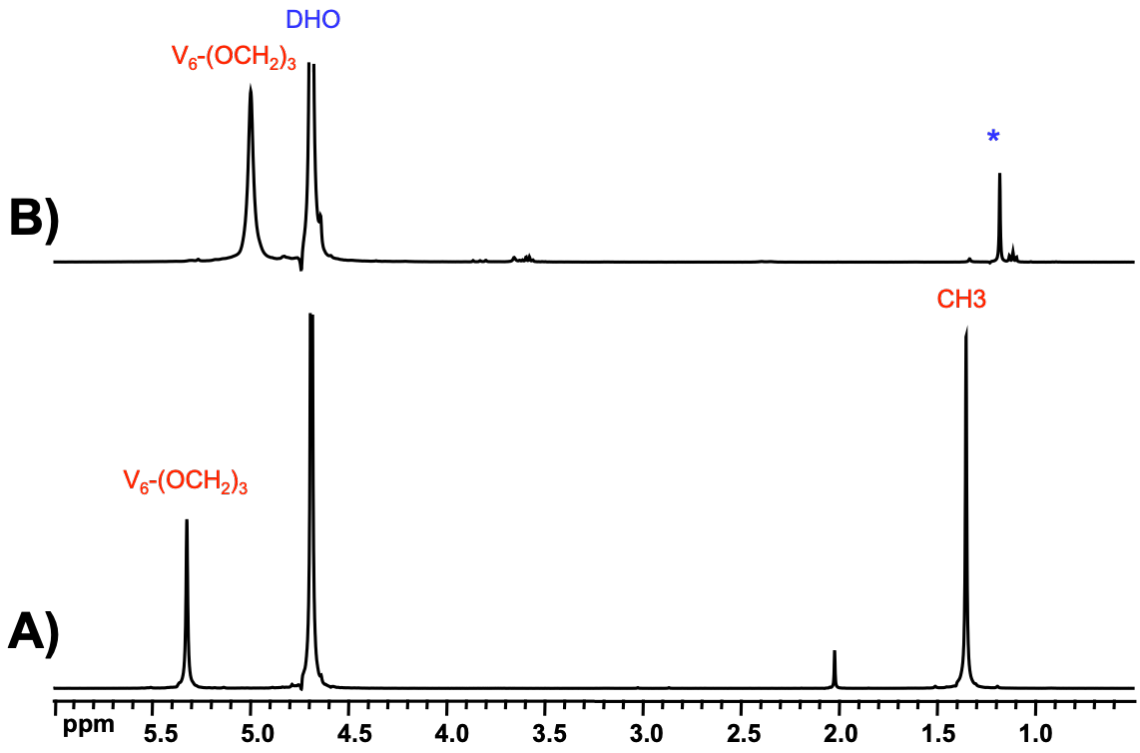

Figure 5: ^1H NMR spectra of A) $Na_2[V_6O_{13}\{(OCH_2)_3C\text{-}NH(BOC)\}_2]$ in D_2O and B) $[V_6O_{13}\{(OCH_2)_3C\text{-}NH_3\}_2]$ in $D_2O/NaOD$. (*) denotes residual BOC (7%).

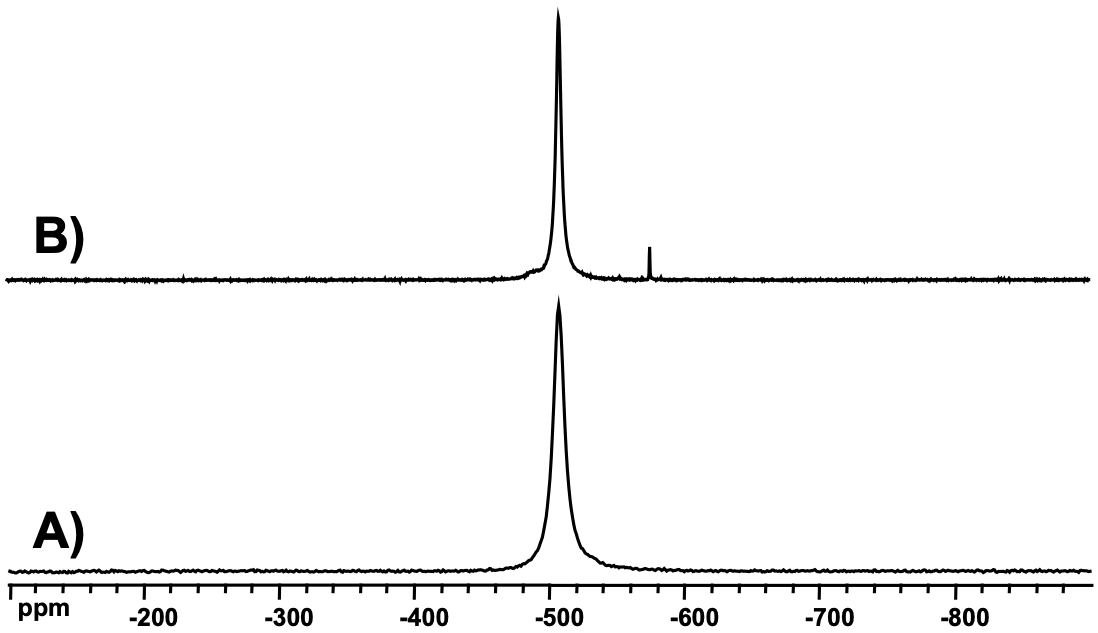

Figure 6: ^{51}V NMR spectra of A) $Na_2[V_6O_{13}\{(OCH_2)_3C\text{-}NH(BOC)\}_2]$ in D_2O and B) $[V_6O_{13}\{(OCH_2)_3C\text{-}NH_3\}_2]$ in D_2O/NaOD.

3.5. UV-vis spectroscopy

The UV-vis spectrum of the $[V_6O_{13}\{(OCH_2)_3C\text{-}NH(BOC)\}_2]^{2-}$ have been measured in acetonitrile using the TBA^+ salt. This spectrum exhibits two strong absorption bands located at 262 nm and 365 nm (Figure 7), and the corresponding molar extinction coefficient are 20300 and 8465 M^{-1} cm^{-1}, respectively. These values are in the same range than those observed by Zubieta on various hexavanadates [19]. These absorption bands are attributed to the oxygen to metal charge transfer transition. The UV-vis spectrum of the $[V_6O_{13}\{(OCH_2)_3C\text{-}NH(BOC)\}_2]^{2-}$ have been also measured in aqueous media using the sodium salt. The spectrum exhibits similar features even if a slightly red-shift (+10 nm) is observed, indicating a solvent dependence of the positions the bands.

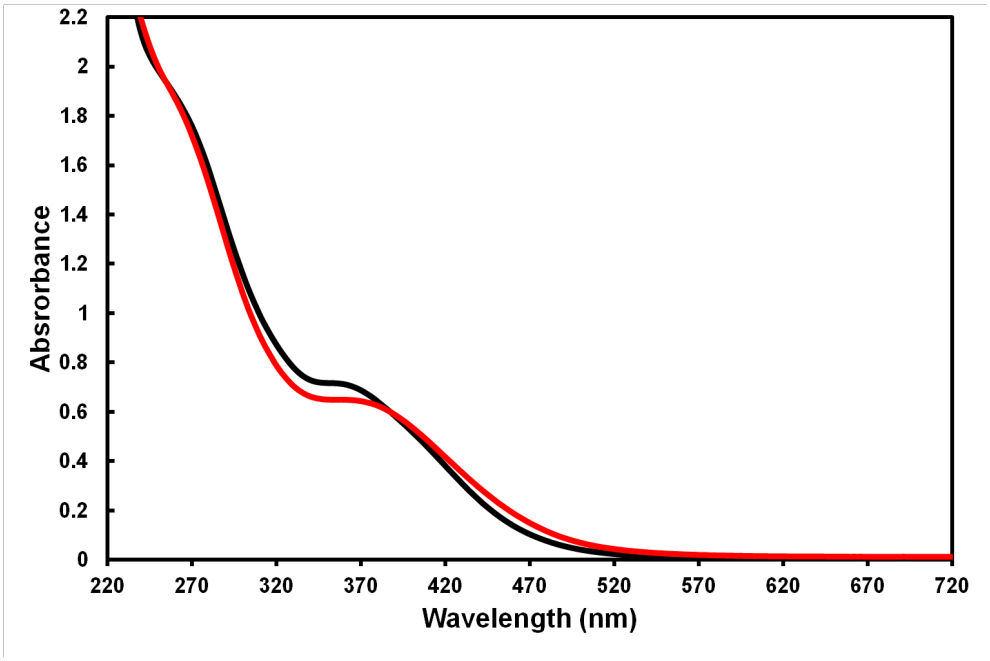

Figure 7 : UV-vis spectra of $TBA_2[V_6O_{13}\{(OCH_2)_3C\text{-}NH(BOC)\}_2]\bullet 2DMA$ in MeCN (black line) $Na_2[V_6O_{13}\{(OCH_2)_3C\text{-}NH(BOC)\}_2]\bullet 6H_2O$ in water (red line).

4. Conclusion

We have synthesized a new tris(hydroxymethyl)aminomethane (Tris) based functionalized Lindqvist-type hexavanadate, $TBA_2[V_6O_{13}\{(OCH_2)_3C\text{-}NH(BOC)\}_2]$, using N-tert-butoxycarbonyl (BOC) as protecting group of the Tris amine function. The compound has been characterized by single crystal XRD and FT-IR spectroscopy in the solid state as well as UV-vis and multinuclear NMR spectroscopies in solution. The sodium salt obtained by cationic exchange is found highly soluble and stable in aqueous solution, which allows deprotection of the amine group to obtain the dianion $[V_6O_{13}\{(OCH_2)_3C\text{-}NH_2\}_2]^{2-}$. This new synthetic method offers simplified procedure for obtaining Tris-Lindqvist vanadate anion with good yield.

Acknowledgment

Authors gratefully acknowledge financial support from LabEx CHARMMMAT (grant number ANR-11-LBX-0039). This work was also supported by i) University of Versailles Saint Quentin, ii) CNRS, iii) Région Ile de France through DIM Nano K. Ibrahima Fa Bamba and E. C. thanks the Embassy of Ivory Coast in France for its scholarship. M. Frigoli (ILV) is acknowledged for fruitful discussions.

References

[1] J. Livage. *Coord. Chem. Rev.*, **178**, 999, (1998).
[2] K.Y. Monakhov, W. Bensch, P. Kogerler. *Chem. Soc. Rev.*, **44**, 8443, (2015).

[3] L.E. VanGelder, T.R. Cook, E.M. Matson. *Comments Inorganic Chem.*, **39**, 51, (2019).
[4] L.E. VanGelder, A.M. Kosswattaarachchi, P.L. Forrestel, T.R. Cook, E.M. Matson. *Chem. Sci.*, **9**, 1692, (2018).
[5] L.E. VanGelder, B.E. Petel, O. Nachtigall, G. Martinez, W.W. Brennessel, E.M. Matson. *ChemSusChem*, **11**, 4139, (2018).
[6] L.E. VanGelder, E. Schreiber, E.M. Matson. *J. Mater. Chem. A*, **7**, 4893, (2019).
[7] J.J. Chen, M.D. Symes, S.C. Fan, M.S. Zheng, H.N. Miras, Q.F. Dong, L. Cronin. *Adv. Mater.*, **27**, 4649, (2015).
[8] J.J. Chen, J.C. Ye, X.G. Zhang, M.D. Symes, S.C. Fan, D.L. Long, M.S. Zheng, D.Y. Wu, L. Cronin, Q.F. Dong. *Adv. Energy Mater.*, **8**, 6, (2018).
[9] S. Greiner, M.H. Anjass, M. Fichtner, C. Streb. *Inorg. Chem. Front.*, **7**, 134, (2020).
[10] S.S. Lu, Y. Lv, W.Q. Ma, X.F. Lei, R.E. Zhang, H. Liu, X.Z. Liu. *Inorg. Chem. Front.*, **4**, 2012, (2017).
[11] B. Schwarz, J. Forster, M.H. Anjass, S. Daboss, C. Kranz, C. Streb. *Chem. Commun.*, **53**, 11576, (2017).
[12] B. Schwarz, J. Forster, M.K. Goetz, D. Yucel, C. Berger, T. Jacob, C. Streb. *Angew. Chem.-Int. Edit.*, **55**, 6329, (2016).
[13] C. Li, N. Mizuno, K. Murata, K. Ishii, T. Suenobu, K. Yamaguchi, K. Suzuki. *Green Chem.*, 10.1039/D0GC01500H, (2020).
[14] B.E. Petel, W.W. Brennessel, E.M. Matson. *J. Am. Chem. Soc.*, **140**, 8424, (2018).
[15] B.E. Petel, A.A. Fertig, M.L. Maiola, W.W. Brennessel, E.M. Matson. *Inorg. Chem.*, **58**, 10462, (2019).
[16] B.E. Petel, R.L. Meyer, M.L. Maiola, W.W. Brennessel, A.M. Muller, E.M. Matson. *J. Am. Chem. Soc.*, **142**, 1049, (2020).
[17] A.V. Anyushin, A. Kondinski, T.N. Parac-Vogt. *Chem. Soc. Rev.*, **49**, 382, (2020).
[18] J.W. Zhang, Y.C. Huang, G. Li, Y.G. Wei. *Coord. Chem. Rev.*, **378**, 395, (2019).
[19] Q. Chen, D.P. Goshorn, C.P. Scholes, X.L. Tan, J. Zubieta. *J. Am. Chem. Soc.*, **114**, 4667, (1992).
[20] J.W. Han, K.I. Hardcastle, C.L. Hill. *Eur. J. Inorg. Chem.*, 2598, (2006).
[21] D. Li, J. Song, P.C. Yin, S. Simotwo, A.J. Bassler, Y.Y. Aung, J.E. Roberts, K.I. Hardcastle, C.L. Hill, T.B. Liu. *J. Am. Chem. Soc.*, **133**, 14010, (2011).
[22] P.C. Yin, A. Bayaguud, P. Cheng, F. Haso, L. Hu, J. Wang, D. Vezenov, R.E. Winans, J. Hao, T. Li, Y.G. Wei, T.B. Liu. *Chem.-Eur. J.*, **20**, 9589, (2014).
[23] P.C. Yin, J. Wang, Z.C. Xiao, P.F. Wu, Y.G. Wei, T.B. Liu. *Chem.-Eur. J.*, **18**, 9174, (2012).
[24] P.C. Yin, P.F. Wu, Z.C. Xiao, D. Li, E. Bitterlich, J. Zhang, P. Cheng, D.V. Vezenov, T.B. Liu, Y.G. Wei. *Angew. Chem.-Int. Edit.*, **50**, 2521, (2011).
[25] Y.T. Zhu, Y.C. Huang, Q. Li, D.J. Zang, J. Gu, Y.J. Tang, Y.G. Wei. *Inorg. Chem.*, **59**, 2575, (2020).
[26] Q. Chen, J. Zubieta. *Inorg. Chim. Acta*, **198**, 95, (1992).
[27] Q. Chen, J. Zubieta. *Inorg. Chem.*, **29**, 1456, (1990).
[28] A. Müller, J. Meyer, H. Bögge, A. Stammler, A. Botar. *Z. Anorg. Allg. Chem.*, **621**, 1818, (1995).
[29] A. Bayaguud, K. Chen, Y.G. Wei. *Nano Res.*, **9**, 3858, (2016).
[30] Z.C. Xiao, K. Chen, B.L. Wu, W.J. Li, P.F. Wu, Y.G. Wei. *Eur. J. Inorg. Chem.*, 808, (2016).
[31] A. Bayaguud, J. Zhang, R.N.N. Khan, J. Hao, Y.G. Wei. *Chem. Commun.*, **50**, 13150, (2014).
[32] B.F. Zhang, J. Song, D. Li, L. Hu, C.L. Hill, T.B. Liu. *Langmuir*, **32**, 12856, (2016).
[33] A. Bayaguud, K. Chen, Y.G. Wei. *Crystengcomm*, **18**, 4042, (2016).
[34] U. Ragnarsson, L. Grehn. *RSC Adv.*, **3**, 18691, (2013).
[35] J. Selambarom, S. Monge, F. Carre, J.P. Roque, A.A. Pavia. *Tetrahedron*, **58**, 9559, (2002).
[36] V.W. Day, W.G. Klemperer, D.J. Maltbie. *J. Am. Chem. Soc.*, **109**, 2991, (1987).
[37] R. Kaplanek, T. Briza, M. Havlik, P. Martasek, V. Kral. *J. Fluor. Chem.*, **128**, 179, (2007).
[38] O.V. Dolomanov, L.J. Bourhis, R.J. Gildea, J.A.K. Howard, H. Puschmann. *J. Appl. Crystallogr.*, **42**, 339, (2009).
[39] G.M. Sheldrick. *Acta Crystallogr. Sect. C-Struct. Chem.*, **71**, 3, (2015).
[40] G.M. Sheldrick. *Acta Crystallogr. Sect. A*, **71**, 3, (2015).

[41] M.A. Delsuc, T.E. Malliavin. *Anal. Chem.*, **70**, 2146, (1998).